

**FIFTH INTERNATIONAL CONGRESS ON SOUND AND VIBRATION**

DECEMBER 15-18, 1997  
ADELAIDE, SOUTH AUSTRALIA

**Diagnosis for Radial Rolling Contact Bearing  
using Acoustic Emission Technique  
(1st Report) : Acoustic Emission Source Location Method**

T. Yoshioka<sup>a</sup> and H. Mano<sup>b</sup>

<sup>a</sup> Machine Elements Division, Mechanical Engineering Laboratory,  
1-2, Namiki, Tsukuba, Ibaraki, 305 JAPAN

<sup>b</sup> Department of Mechanical System Engineering, Tokyo University of Agriculture  
and Technology, 2-24-16, Naka-cho, Koganei, Tokyo, 184 JAPAN

## **ABSTRACT**

This paper describes the principle of an acoustic emission (AE) source location method for a radial rolling bearing and proof of the location method. The method locates contact points between balls and an inner ring within a loading zone of a radial rolling bearing under a radial load at the moment of AE generation as possible AE sources. The location result in which the X-axis shows the position on a raceway of the inner ring and the Y-axis is the cumulative AE events, is shown as a histogram which has several peaks and is symmetrical at the highest peak after locating repeatedly. In the location result, the position of the highest peak agrees with the position of the actual AE source.

The principle of the location method was proven by rolling contact fatigue tests using radial ball bearings. The locator was comprised of AE measurement system and position detectors of the inner race and the balls. The AE sensor and the detection sensors were fixed on the housing of the test bearing. The locator in the system decided the source position of AE under signals from the system and the detectors. The positions located by the method agreed with the positions of spallings. It was confirmed in the rolling contact fatigue tests that AE was caused by propagation of rolling contact fatigue crack and occurred before the appearance of spalling.

## **1. INTRODUCTION**

In terms of the conservation of energy and resources, and preservation of the environment, it is necessary to operate machinery safely and efficiently. A huge number of rolling bearings have been used to support rotational axes and oscillating axes in machinery and have sometimes failed during operation of machinery. Therefore, it has become more important to monitoring the condition of a rolling bearing.

There has been a lot of research on detection and diagnosis of bearing failures by

vibration, acoustic emission (AE), wear particle analysis, etc.. The detection of rolling bearing failure using AE techniques was reported by R. James et al.[1] in 1973. They observed the trend of AE root-mean-square (r.m.s.) value and amplitude distribution of AE, and discovered that the AE r.m.s. value increased and amplitude distribution changed when failure occurred in a bearing. L. C. Ensor et al.[2] detected AE emitted from a radial ball bearing in operation, however they could not make clear the cause of AE. T. Yoshioka and T. Fujiwara[3] developed an AE source location method which decided the positions of balls on the raceway at the moment of AE generation as possible AE source positions and applied it to a test bearing which simulated a thrust ball bearing. It was found from the results of rolling contact fatigue tests that AE was generated at spalling position before spalling[4,5,6] and the r.m.s. value of vibration increased when spalling appeared in the raceway surface[7].

The diagnosis for a radial bearing has never been developed, because the cause of AE emitted from the bearing was not clarified and AE caused by failure could not be discriminated from noise. In order to make clear the cause of AE, we think that it is an important technique to locate AE source position. However, any methods which locate AE source position for a radial bearing have not been developed.

A new AE source location method for a radial bearing is proposed and examined by rolling contact fatigue tests in this paper. The method is very important to understand correctly the activity of a rolling fatigue crack as well as discrimination of noise. To understand the activity of a fatigue crack is essential for the establishment of predictive maintenance of a rolling bearing.

## 2. PRINCIPLE OF AE SOURCE LOCATION METHOD

The developed AE source location method locates contact points between balls and an inner ring within a loading zone of a radial rolling bearing under a pure radial load at the moment of AE generation as possible AE sources. The location method requires signals relating to the position on the inner raceway and the position of a ball as well as acoustic signals.

An another AE location method has plural AE sensors and calculates the AE source positions by the difference of arrival time of an acoustic signal at each sensor. The method has been used in many research fields to locate the AE source position. However, the resolution of the location method is lower, because the shape of AE signal is disordered during propagation from the AE source to sensors. For this reason, the above method is not necessarily suitable when applied to rotational machine elements.

Figure 1 shows the arrangement of a test bearing and the sensors of the new location method. The test bearing is a deep groove ball bearing. Eight balls are assembled in it. The AE sensor is fixed on the housing of the test bearing. The inner ring position sensor is attached on the O-Y axis and generates a signal to measure the inner ring position when the marker on the inner race passes through in front of it. The ball position sensor is on the pitch circle of the test bearing clockwise at the angle of  $\phi$  around O from the O-Y axis and detects passage of a ball. A loading zone is induced in the test bearing between the angle of  $\pm \theta$  around the maximum rolling element load position (O-Y' axis) when the pure radial load is applied to it.

The AE location method for an inner race decides the points on the inner raceway which come into contact with balls within the loading zone at the moment of AE generation as

possible AE source positions. It is assumed that AE occurs at each time when the inner ring comes into contact with the balls as shown in Figure 2 (i) and (ii).  $\omega_i$  is a rotational angular velocity of the inner ring and  $\omega_r$  is a revolutionary angular velocity of the ball set.  $t_1$  and  $t_2$  are the times from passage of the marker on the inner ring in front of the inner ring position sensor to each AE generation, respectively. And  $t_{r1}$  and  $t_{r2}$  are the times from passage of a ball in front of the ball position sensor to each AE generation, respectively. The possible AE source positions are the points a, b, c and d at the AE generation of Fig. 2 (i), and the points c, d and e at the generation of Fig. 2 (ii).

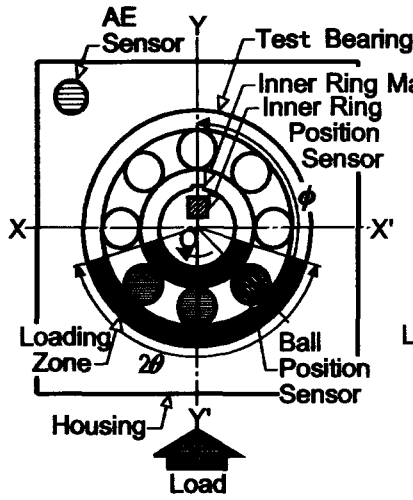


**Figure 1 Arrangement of Test Bearing and Sensors**

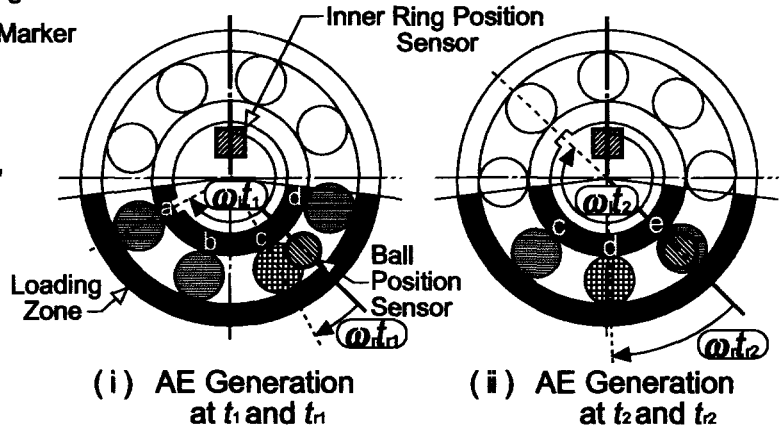


**Figure 2 Contact Conditions of Inner Ring and Balls at AE generation**

The possible AE source positions on the inner raceway are calculated as follows.

In the case of AE generation at the time  $t_k$  after passage of the marker on the inner ring in front of the inner ring position sensor, the rotational angle  $\alpha$  of the marker can be expressed as Equation (1).

$$\alpha = \omega_i t_k \quad (1)$$

The loading zone  $\beta$  of the inner ring corresponding to the rotation of the inner ring can be expressed as Equation (2).

$$180 - \alpha - \theta \leq \beta \leq 180 - \alpha + \theta \quad (2)$$

The revolutionary angle of each ball  $\gamma$  within the loading zone is shown as Equation (3) at the moment of the time  $t_{m}$  which is the elapsed time since a ball passed through in front of the ball position sensor.

$$\gamma = \omega_r t_m + 360 n / z + \phi \quad (3)$$

Here,  $n$  is an integer between  $-1$  and  $z / 2 - 1$ .

The possible AE source positions are the points which satisfy these three equations.

The process of the AE location is illustrated in Fig. 3 as a histogram. The X-axis of Fig. 3 indicates positions on the inner raceway and the Y-axis the cumulative number of AE events. At the first AE generation of  $t_k = t_1$ , one event is added to the position a, b, c and d as shown in Fig. 3 (i), respectively. In the second generation of  $t_k = t_2$ , one event is added to the position c, d and e as shown in Fig. 3 (ii). After many repetitions, we could obtain a histogram like as shown in Fig. 3 (iii). The histogram has the highest peak and plural peaks symmetrically in it. From the location result, the position of the actual AE source on the inner raceway is presumed to be the position of the highest peak of the histogram.

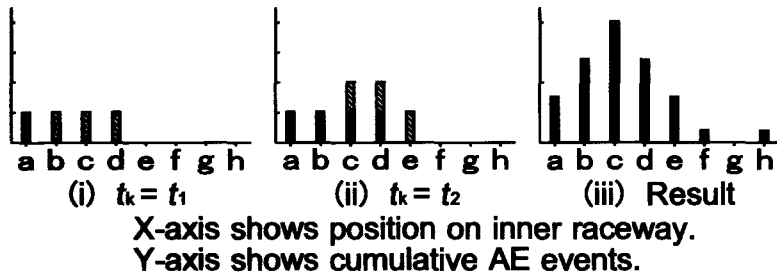


Figure 3 Location Process of Inner Ring

### 3. ROLLING CONTACT FATIGUE TESTS

The bearing testing machine used in the rolling contact fatigue tests is illustrated in Figure 4. A main shaft was supported by two deep groove ball bearings and the test bearing was attached to the end of the shaft. A pulley driven with a motor through v-belt was fixed at the other end. The load was statically applied to the test bearing by means of a dead weight lever system as a pure radial load.

The block diagram in Figure 5 shows an AE and vibration measurement system, including a developed AE source locator. An AE sensor, position sensors which detect rotation of the inner ring and revolution of the ball set and a vibration sensor were fixed on the bearing testing machine. The inner ring position sensor was fixed on O-Y axis and the ball position sensor was fixed at the angle of  $\phi = 135$  degrees around O from O-Y axis on the pitch circle of the test bearing as shown in Fig. 1. The signals detected by the AE sensor, the inner ring position sensor and the ball position sensor were sent to the locator. The locator decided the possible AE source positions according to these signals at every AE generation during the fatigue test, and the location results cumulated for each 5 min were memorized in the personal computer temporarily. The vibration acceleration detected by the vibration sensor was processed to a r.m.s. value in the vibrometer. When the r.m.s. value of vibration exceeded a preset level which depended on a spalling appearance in the fatigue test, a relay circuit of the vibrometer stopped the bearing testing machine automatically. Moreover, the locator which received the output of the relay circuit made the personal computer save the location results for 2 h 30 min just before the spalling appearance.

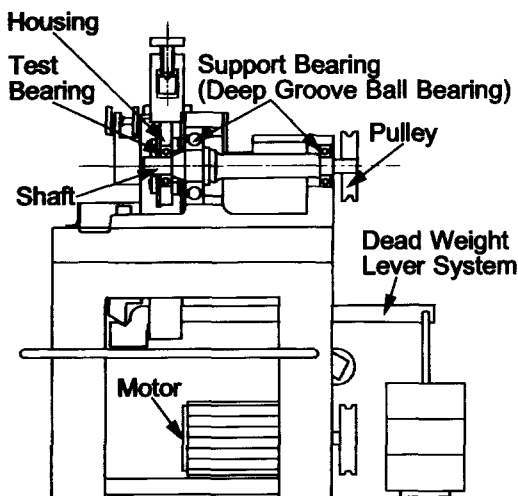


Figure 4 Bearing Testing Machine

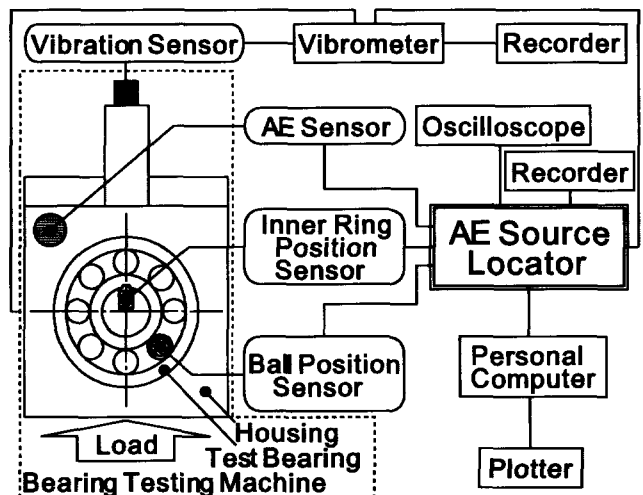


Figure 5 AE and Vibration Measuring System and AE Source Locator

The test bearing simulated a deep groove ball bearing #6204. The balls rolled on the inner raceway without groove shoulders in order to increase stress in a contact surface and accelerate the fatigue test. The inner ring, the outer ring and the balls were made of vacuum-degassed AISI 52100 steel, while the material of the cage was AISI 304.

The test bearing was run under a pure radial load 2.11 kN at a rotational speed 2520 rpm and lubricated with mineral oil corresponding to ISO VG 56. The maximum Hertz contact stress induced in the contact surface between the inner raceway and a ball was 6.51 GPa. In this case, as the loading zone was  $\pm 75$  degrees around the maximum rolling element load position, the value was set in the locator. The fatigue test was automatically terminated as soon as the r.m.s. value of the vibration acceleration exceeded  $7.8 \text{ m/s}^2$ . A test time was recorded by an integrating timer connected with the electric circuit of a motor.

The AE measuring conditions were as follows : the resonance frequency of the AE sensor was approximately 320 kHz, the frequency bandwidth was from 200 kHz to 400 kHz, the amplification degree was 70 dB, and threshold level for the event rate and the location was 1.0 V. The possible AE source positions were located by dividing the inner raceway into 80 equal parts. The whole inner raceway length was approximately 83.3 mm, and the resolution of the locator was approximately 1.04 mm. The vibration acceleration was detected through the frequency bandwidth from 10 Hz to 20 kHz.

#### 4. Experimental Results and Discussion

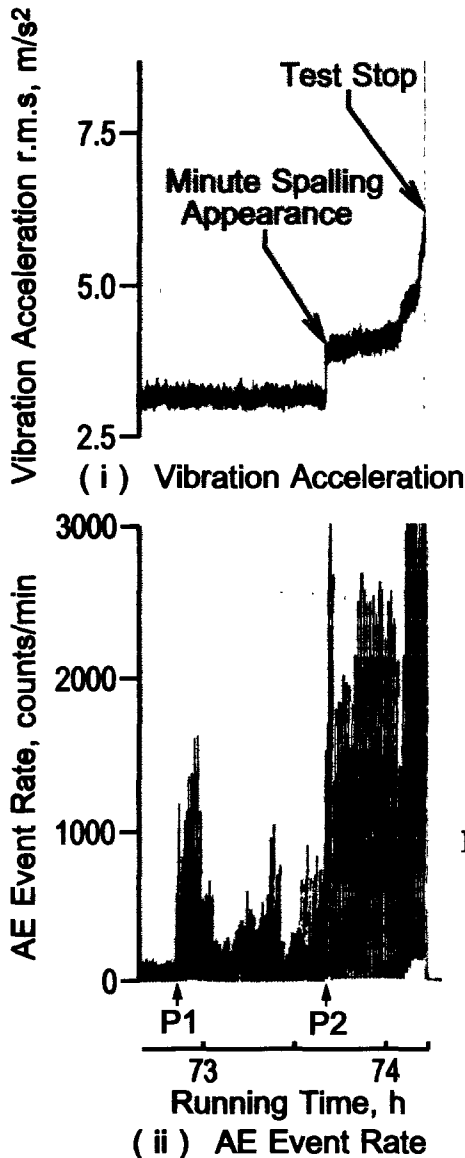
Eight rolling contact fatigue tests were run for AE source location of a radial ball bearing.

Figure 6 shows an example. In the case of the test bearing M-16 which was stopped at 74.3 h, there were certain trends in the vibration acceleration and the AE event rate. The X-axis indicates the running time in hours and the Y-axis is the r.m.s. value of the vibration acceleration in  $\text{m/s}^2$  and the AE event rate in counts/min, respectively. The r.m.s. value increased in a stage at the point of time P2 corresponding to 73.7 h in Fig. 6 (i), when a minute spalling appeared in the surface of the inner raceway. On the other hand, it could be seen in Fig. 6 (ii) that many AE were generated from the point of time P1 of 72.9 h before the spalling.

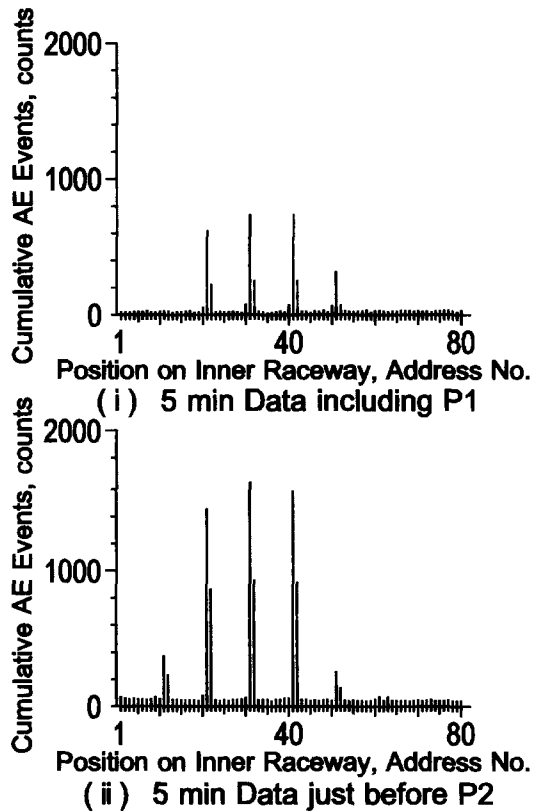
Figure 7 illustrates the location results of the AE source position on the inner raceway of M-16. All AE generated for 5 min including the time P1 and just before the time P2 were cumulated in the location results. The X-axis indicates the position on the inner raceway in an address scale from 1 to 80 and the Y-axis indicates the cumulative AE events in counts for 5 min. We can see in Fig. 7 that several peaks appeared at the interval of 10 addresses. The highest peak was at the address No. 31 on the inner raceway and the position of the highest peak was decided as the actual AE source position. The spalling position on the inner raceway was measured after fatigue test, and it was confirmed that the spalling position agreed with the located position. In addition, the same position was always located in the period from the time P1 to the time P2. Therefore, the AE detected in this period was presumed to be caused by the propagation of the rolling contact fatigue crack below the surface of the spalling position. Moreover, the time from P1 to P2 was 0.8 h, and it was considered that this time was equal to the propagating time of the fatigue crack.

Figure 8 shows the spalling which appeared at address No. 31 on the inner raceway in this test.

The histogram in Fig. 7 (i) differed from the theoretical result as the located histogram was not symmetric about the highest peak. This difference suggested that the fatigue crack did not always propagate at every contact in the loading zone and propagated when the position of the crack came into contact with a ball before the maximum rolling element load position. Then, a few peaks appeared around each possible AE source position in Fig. 7. The reason for this was considered to be an error between a detected position and an actual contact position. The ball position was detected according to the outer surface of a cage in practice. Therefore, the error appeared due to the relative motion of the cage to the balls, because a clearance existed between the cage pockets and the balls.



**Figure 6** Trend of Vibration Acceleration and AE of Test Bearing M-16



**Figure 7** Location Results of Test Bearing M-16



**Figure 8** Spalling at Address No. 31 on Inner Raceway of Test Bearing M-16

Figure 9 shows another example. In the case of the test bearing M-21 which was stopped at 159.5 h, there were certain trends in the vibration acceleration and the AE event rate. The r.m.s. value of the vibration acceleration increased stepwise at the point of time P2 corresponding to 159.2 h by the minute spalling appearance in Fig. 9 (i). On the other hand,

it could be seen in Fig. 9 (ii) that many AE were generated from the point of time P1 of 159.0 h before the minute spalling appeared. Figure 10 illustrates the location result of the AE source position on the inner raceway of M-21 and all AE generated for 5 min including the time P1 were cumulated in it. The address No. 52 on the inner raceway was located as an actual AE source position by the histogram. It was confirmed that the located position agreed with the measured spalling position on the inner raceway accurately. Therefore, the time of 0.2 h from P1 to P2 was equal to the propagating time of the fatigue crack. Figure 11 shows the spalling at address No. 52 on the inner raceway.

If considered from a different standpoint, it was concluded that the propagating time of the fatigue crack corresponded to the predictive time of the spalling appearance.

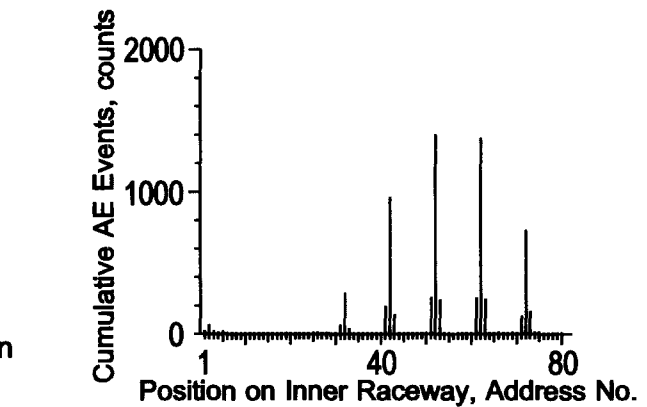
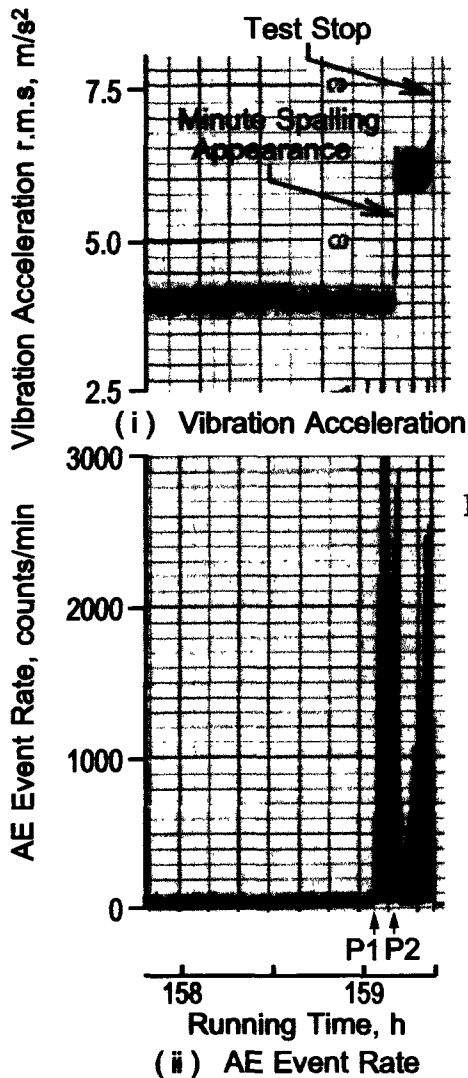


Figure 10 Location Result of Test Bearing M-21

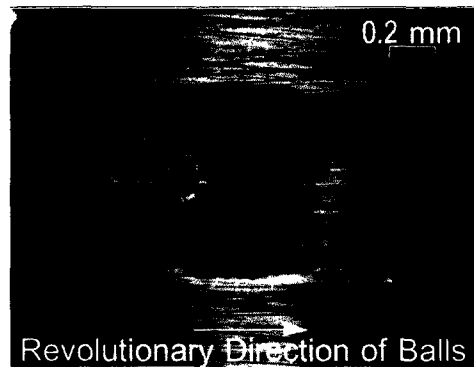
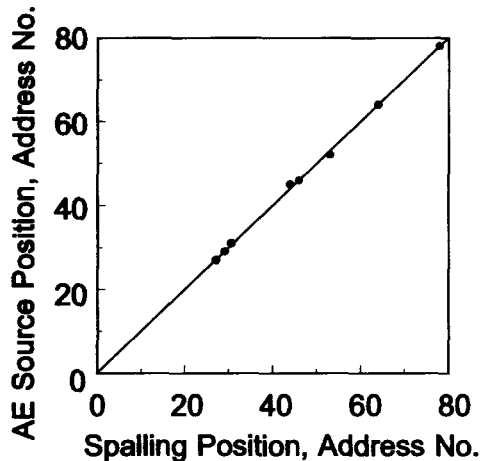


Figure 11 Spalling at Address No. 52 on Inner Raceway of Test Bearing M-21

Figure 9 Trend of Vibration Acceleration and AE of Test Bearing M-21

Figure 12 illustrates the relationship between the located address of the AE source position and the measured address of the spalling position in eight fatigue tests. The solid line of 45 degrees in Fig. 12 shows the correlation coefficient of 1. The plots obtained by the experiments are distributed near the solid line within the limits of  $\pm 1$  address. Accordingly, it was proven that the proposed method could locate the AE source position correctly, accurately and with good reproducibility.



**Figure 12 Relationship between AE Source Positions and Spalling Positions of Inner Ring**

## 5. SUMMARY

We have developed a new location method of AE source for a radial rolling bearing. The method located contact points between balls and an inner raceway within a loading zone at the moment of AE generation as possible AE source positions. The following results were obtained in rolling contact fatigue tests :

1. The located AE source positions agreed with spalling positions. And the method located the AE source positions within  $\pm 1$  address of the spalling positions. Therefore, it was proven by the fatigue tests that the proposed location method was correct and accurate.
2. It was made clear that the propagating times of rolling contact fatigue cracks could be measured for radial rolling bearings.
3. The rolling contact fatigue crack of the inner raceway did not always propagate if the position of crack came into contact with balls within the loading zone.

It is our intention to measure the propagating times of rolling contact fatigue cracks for radial rolling bearings in order to establish predictive maintenance of rolling bearings.

## REFERENCES

- [1] R. James, B. Reber, B. Baird and W. Meal, The Oil and Gas Journal, 72, Dec. (1973) 49.
- [2] L. C. Ensor, C. C. Feng, R. M. Whittier and A. D. Diercks, NASA Contract NAS 8-29916, (1975).
- [3] T. Yoshioka and T. Fujiwara, ASME PED-Vol. 14, (1984) 55.
- [4] T. Yoshioka and T. Fujiwara, Tribology Series, 12, Interface Dynamics, Elsevier, (1988) 29.
- [5] T. Yoshioka, Lubrication Engineering, 49, 4 (1993) 303.
- [6] T. Yoshioka and M. Takeda, Lubrication Engineering, 51, 1 (1995) 41.
- [7] T. Yoshioka, Japanese Journal of Tribology, 34, 12 (1989) 1405.